RELIABILITY OF STEEL BEAM-TO-COLUMN CONNECTIONS UNDER CYCLIC LOADING

by

E P. Popov[I] and R. B. Pinkney[II]

SYNOPSIS

The principal findings of an experimental program with steel cantilever beams attached by different types of connections to column stubs and loaded cyclically at the free end are described. The loadings used were chosen to simulate the effect of an earthquake on the joints in a rigid frame steel building. The significance and analytic idealizations of the load-deflection hysteresis loops are discussed in detail. Some data on the capacity of steel beams and their connections as energy dissipators during plastic straining are given.

INTRODUCTION

During a seismic disturbance, building frames are subjected to repeated and reversed lateral loadings. For strong motion earthquakes, portions of the structural frame become critically stressed and behave inelastically during the loading process. For the aseismic design of buildings, it is important to determine the behavior of such critically stressed elements. Since this problem is very complex, analytical procedures alone are inadequate, and laboratory experiments must be performed to obtain the required information. Such an approach requires the selection of appropriate specimens isolated from the structural frame as a whole. This problem was resolved differently by different investigators.

The behavior of a building frame during a severe earthquake is shown schematically in Figs. 1(a) and (b). The heavy dots on these diagrams represent the possible regions of inelastic action. In extreme cases, some of these locations may tend to become plastic hinges.

Experimentation with complete frames such as shown in Figs. 1(a) and (b) is very expensive, and most of the work to date has been on selected components. Some of the typical component testing done in Japan (1, 2, 3) is illustrated in Figs. 1(c), (d), and (e). By applying repeated and reversed loadings to the specimens, the required information is obtained. Note that the specimens of the type shown in Figs. 1(c) and (e) are subjected not only to bending but must also resist substantial axial loads. Inelastic action either in the beam or on the column is possible.

A somewhat different philosophy has been adopted in selecting the specimens described in this paper. As this was the first systematic

---

I Professor of Civil Engineering, University of California, Berkeley, California, U. S. A.

II Graduate student and Research Assistant, University of California, Berkeley, California, U. S. A.

study in the U. S. A. of structural steel connections for buildings under intense repeated and reversed loadings, the number of variables was kept to a minimum. In conformity with the current American design practice, the possibility of plastic action in the columns was excluded from consideration. Further, the dead load stresses were relegated to the place of secondary importance. On this basis the assumed frame behavior during an earthquake is as shown in Figs. 2(a) and (b). The inelastic action is confined to the beams in the regions adjoining columns (shown by heavy dots in the figure). The columns themselves are assumed to remain elastic. This approach logically leads to the type of specimen shown in Fig. 2(c). Because of the simplicity of the chosen specimen it was possible to investigate several types of widely used connections under a variety of loading conditions. In the next generation of experiments already completed or in progress, at the University of California (4) and at Lehigh (5), the behavior of subassemblages and complete frames is being studied. The latter research is not the subject of this paper.

EXPERIMENTAL PROCEDURE AND SUMMARY OF RESULTS

In the course of this research, 24 specimens of the designs shown in Figs. 3(a), (b), (c), and (d) were fabricated and tested. In all of these the cantilever beams were made of 8 WF 20 sections. This section has the b/t ratio similar to that of representative floor beams in high-rise buildings, and its size is sufficiently large to require no special fabrication procedures. All of the connection details were chosen for their practicability and were of the types widely used in practice. In the specimens of the F1 type the beams were welded directly to the column stubs. Connecting plates were used in the other three. In the specimen of the F3 type the beam was attached by means of high-strength bolts.

In several of the specimens of the F2 and F3 types the thickness of the connecting plates was varied. Thus, specimens designated as F2A and F3A had connecting plates 1/16 in. thinner than those shown for F2 and F3 respectively. For specimens F2B and F3B the connecting plates were 1/8 in. less than the corresponding plates of specimens F2 and F3. Specimens similar to W1 but having tapered or shaped connecting plates were designated as W2.

A total of twenty specimens using A-36 steel were fabricated according to the above details. Four additional specimens of the F1 and F2 types were made of A-441 steel. These are identified by letters HS and are referred to as F1HS and F2HS. A more detailed description of these specimens may be found elsewhere (6, 7, 8).

A specimen made of A-36 steel having the detail shown in Fig. 3(e) was designated as LA1. The beam in this assembly was made by continuously welding together three plates to form an I-section. The web of this beam was bolted to the shear plate and the flanges were welded to the column stub. This specimen was a one-third scale model for a projected building in the Los Angeles area. This connection utilizes erection bolts for shear transfer and welding to transfer moment. It is advantageous from the cost point of view. An identical beam with two outer bolts in the shear connection removed was designated as LA2.

All of the specimens enumerated above have been tested one at a time in a fixture shown in the photograph of Fig. 4. In each case the column stubs were bolted to the test frame and a double acting hydraulic cylinder provided the concentrated load input at the tip of the cantilever. To prevent lateral buckling of the beam, guides at the center and at the end were provided (6, 7, 8).

Experiments were controlled either by a strain gage near the built-in end of the cantilever or by a selected tip deflection. Some typical loading programs are shown in Fig. 5. In Fig. 5(a) the multiple step sequence of applying progressively larger and larger tip deflections is illustrated. This type of cycling sequence was used particularly often. In Fig. 5(b) essentially the same type of cycling program is illustrated, but is begun by a few cycles of very large amplitude. The cycling sequence shown in Fig. 5(c) resulted from following a prescribed strain history in the control gage on the top of the beam.

The various types of cycling sequenced were designated as C1, C2, C3, C4, etc. This permitted the identification of each specimen by its type and the nature of the cycling program as F1-C1, etc. The one specimen which was tested without subjecting it to the reverse cyclic loading was designated as F1-S.

In every experiment with cyclic load sequence, the work was terminated only after an actual failure of the member had occurred. A few photographs of some specimens after failure are shown in Figs. 6, 7, 8, and 9. The performance of specimens together with their loading history is summarized in Tables I and II. In examining the photographs and the tables it must be recognized that the cycling sequences were chosen arbitrarily. Moreover, the strain levels reached in the beams and the connecting plates are of a very great severity, which normally would not occur in actual building frames. On the other hand, such information is of great value to the designer to show the nature of failure of details. There is always also the possibility that some unfavorably oriented members and connections in an actual building may be subjected to loads beyond those which were anticipated by the designer.

All of the experiments were of the quasi-static type with the loads applied rather slowly. In order to make the required readings before and after each cycle it required two or three days to complete some of the experiments. Therefore, it is reassuring that information so obtained has been shown to be in excellent agreement with dynamic tests (9, 10).

DISCUSSION OF RESULTS

The behavior of specimens is best described by their load-deflection hysteresis loops. These were obtained for nearly all specimens tested under cyclic loading. A study of the hysteretic loops shows the progressive variation in the stiffness of a member, its energy absorption capacity as measured by the area enclosed by the loops, and the nature of residual deflections which may occur.

In the elastic range, in common with other materials, structural steel exhibits a small hysteretic effect. However, as the material is

strained into the plastic or inelastic range, substantial hysteresis loops develop. The shapes of the hysteresis loops for many materials, including those for steels, are well known (11). The distinguishing feature of the loops investigated here is due to the fact that they show more than the properties of the material alone. Since the tests were performed on beams and their connections, the geometric proportions and the manufacturing details of the members play an important role. During severe straining, flanges of the beams can buckle, and numerous locations with locally high stresses are inevitable. The hysteresis loops obtained in these experiments display the above characteristics and reflect the overall behavior of the specimens.

Several salient points regarding the hysteresis loops and the information they provide for the designer are discussed next.

Loop Stability. Several hysteresis loops from different experiments are reproduced in Fig. 10. Originally these loops were obtained automatically using an XY recorder with the signals provided by a linear potentiometer for the tip deflection and a transducer mounted on the hydraulic ram for the load (6, 8). These loops clearly show that if the control conditions are not altered, hysteresis loops of essentially the same shape are obtained during several consecutive cycles. This loop stability for repeated cycles was characteristic of all experiments, although some cyclic softening of the loops was observed in experiments with a large number of cycles at a contest deflection, Fig. 11. Such a large number of cycles appears to have little relevance to the situations likely to occur in structural steel frames during an earthquake. Note from Fig. 11 that for the adjoining cycles the loops are nearly coincident; i.e., they do not deteriorate to any appreciable extent.

It is important to observe that stable loops were obtained for cycles number 6, 7, and 8 for the specimen F1HS-C11. These were obtained after subjecting the specimen to five very severe cycles of load application, Fig. 5(b). The ability of connections to perform well after withstanding intense loadings is highly significant. It must also be emphasized that these experiments demonstrated that buckling of the flanges did not materially deteriorate the loops. During the consecutive cycles the flanges cyclically buckled and then tended to straighten out without substantially reducing the load carrying capacity of the assembly. However, to achieve good results the necessity of proper detailing, inspection, and fabrication cannot be overemphasized. In these experiments two specimens failed prematurely due entirely to poor workmanship (6, 7).

Loop Size. As mentioned earlier, negligibly small hysteresis loops are generated by steel in the elastic range. However, in the inelastic range they develop into a large size. The same is true for the load-deflection hysteresis loops. The size of the loops increases with an increase in the applied load or the induced deflection. Three selected loops at progressively larger loads are shown in Fig. 12. These were typical of welded connections of the general type F1 and F2. Except for being smaller in size, specimens LA1 and LA2 generated similar loops.

The superimposed loops providing a visual comparison of their size are also shown in Fig. 12. A curve drawn through the tips of the loops

gives the so-called skeleton curve which will be discussed further in the sequel.

Loop Clusters. In making use of the hysteresis loops in the analysis of frames the loops as a rule are not located in true antisymmetric manner around the origin. Therefore, it is of some interest to obtain a few loops displaced along the horizontal axis. This was done with the specimen F1-C6. By controlling the experiment by means of a strain gage on the top flange 5 ½ in. from the column, the load-strain input was chosen to be as shown in Fig. 13(a). The resulting load-deflection loops then became as in Fig. 13(b). This experiment provides some degree of confidence in the reliability of calculations which may require the displacement of the hysteresis loops along the abcissa. Future experiments are being planned to explore the nature of hysteresis loops for loads of unequal magnitude in the two opposite directions.

Loops of Irregular Shapes. In some instances very unusual shapes of hysteresis loops were obtained. Some of these are shown in Fig. 14. In Figs. 14(a) and (b) load-deflection loops for the specimen F3-C5 are shown. This was a bolted connection with punched holes 1/16 in. larger than the nominal bolt diameter. Note the distinctly different loop of the first cycle. Before friction is broken in the interstices of the faying surfaces, the loop is not unlike those of the welded specimens. However, in the subsequent cycles several distinct regions of behavior can be recognized. First, the no-slip region can be observed, then the region of interstice slip is clearly seen, and finally the one when the bolts are seated and act in bearing. The size of the loop in this severely strained specimen is quite large.

In another bolted connection, specimen F3A-C7, the holes were drilled and were only 1/64 in. larger than the nominal bolt diameter. The slip region in this connection was dramatically smaller than above as may be seen from Fig. 14(c).

Irregularly shaped loops were also observed in an all-welded connection F2B-C8, Fig. 14(d). In this specimen the connecting plates were chosen undersize and were 1/8 in. thinner than those of the standard F2 type. Here the connecting plates, while in compression, tended to buckle, whereas in tension, a crack in the connecting plate closes first which then stiffens the member.

Results such as these may be useful not only for design of new frames, but also in interpreting damage in the aftermath of an earthquake.

Monotonic Versus Cycling Loading. Engineers are well versed in the elastic and plastic behavior of steel structures under static loads. Transition from an idealized elastic-plastic stress-strain diagram to a moment-curvature diagram and thence to load-deflection diagrams now may be considered completely resolved. Strain hardening can also be adequately treated. By contrast, the relationship between static load-deflection diagrams for monotonically applied loads and the corresponding diagrams for cyclic loading received scant attention. This aspect of the problem is commented upon here.[8]

In Fig. 15 the monotonic and cyclic stress-strain behavior of SAE 4340 steel is shown (11). This diagram clearly indicates cyclic curve to lie below monotonic; in other cases such curves lie above (11). The evidence gathered in these experiments appears to show that the cyclic curve lies above the monotonic one.

In arriving at a cyclic stress-strain curve it must be noted that the virgin branch of the stress-strain curve is excluded, and it is tacitly assumed that the material very rapidly adjusts to a nearly stable steady-state condition. An analogous phenomenon can be noted in the cyclic load-deflection behavior of the specimens described here.

Specimen F1-S was tested by applying the tip load without reversing its direction, although it was unloaded three times during the course of the experiment. The resulting data are accepted here as representative of monotonic loading, Fig. 16. To generate the cyclic load-deflection curve on the same plot, reduced results for F1 type specimens were reviewed. Then by favoring the initial loops for each deflection amplitude, coordinate points defining the tips of the hysteresis loops were selected at random. This data in dimensionless form are plotted as points for estimating the skeleton curve in Fig. 16.

The points enclosed by enlarged circles were excluded in sketching-in the approximate skeleton curve which is also the cyclic load-deflection curve. These points correspond to the situations prevailing at the time of a very large number of cycles, and are not considered of primary importance in this comparison. Points for specimen F1HS-C11 which was subjected initially to very severe cycling were also somewhat discounted. On this basis on a dimensionless plot in Fig. 16 both the A-36 and the A-441 steels exhibit approximately the same behavior, and the cyclic curve is above the monotonic curve.

Analytic idealizations. For the purposes of analyzing the response of a structural steel frame due to an earthquake, it is necessary to formulate some of the above findings in mathematical form. For this purpose the Ramberg-Osgood description (12) for non-linear stress-strain relations can be adopted for the skeleton curves shown in Figs. 12 and 16. This formulation gives

$$\frac{\Delta}{\Delta_p} = \frac{P}{P_p}\left[1 + \alpha \left|\frac{P}{P_p}\right|^{r-1}\right] \qquad (1)$$

where Δ and P are the applied load and deflection respectively and α and r are experimental constants. It is convenient to regard the quantity P_p as the plastic load and to take $\Delta_p = \Delta_y P_p/P_y$ where the subscripts y designate the conditions at yield.

Instead of fitting Eq. 1 to the cyclic experimental load-deflection curves, theoretically it is possible to deduce such an equation directly from cyclic stress-strain relations (13). Such data, however, were lacking in these experiments. A less satisfactory but nevertheless meaningful correlation between the measured moment-curvature and load-deflection

curves has been achieved in these experiments (14). In the analytical form for this purpose one can begin with the Ramberg-Osgood moment-curvature relation, which reads

$$\frac{\varphi}{\varphi_p} = \frac{M}{M_p}\left[1 + \alpha^* \left|\frac{M}{M_p}\right|^{r^*-1}\right] \qquad (2)$$

where φ and M are the curvature and moment, respectively, and α^* and r^* are experimental constants. As before, the subscripts p refer to the condition at impending plastic load.

With $M = Px$ by integrating $x\varphi dx$, which is equivalent to the application of the moment-area method used in Reference 14 after some simplification, one obtains

$$\frac{\Delta}{\Delta_p} = \frac{P}{P_p}\left[1 + \frac{3\alpha^*}{r^* + 2}\left|\frac{P}{P_p}\right|^{r^*-1}\right] \qquad (3)$$

A comparison of this equation with Eq. 1 shows that for this case of a linearly varying moment, $r = r^*$ and $\alpha = 3\alpha^*/(r^* + 2)$. This relationship applies rigorously only before the occurrence of buckling in the flanges. An extension of this theory appears desirable.

By using Eq. 3 or its simpler equivalent, Eq. 1, it is possible to generate analytic expressions for the hysteresis loops by adopting Masing's hypothesis (15). This approach has been used by several investigators (13 and 16). According to this hypothesis the skeleton curve is enlarged by a factor of two, and the point (Δ_i, P_i) is chosen as the point of last load reversal, whence

$$\frac{\Delta - \Delta_i}{2\,\Delta_p} = \frac{P - P_i}{2\,P_p}\left[1 + \alpha\left|\frac{P - P_i}{2\,P_p}\right|^{r-1}\right] \qquad (4)$$

The graphical meaning of this equation has been illustrated in a number of papers (6, 16). It is capable of generating an arbitrary sequence of complete or partial loops as shown in Fig. 17, which is precisely what is needed for the non-linear analysis of frames.

In comparing Eq. 4 with the experimental data it has been found that it gives reasonable results. A more accurate expression, however, would be

$$\frac{\Delta - \Delta_i}{\Delta_p} = \frac{1}{\beta}\frac{P - P_i}{P_p}\left[1 + \alpha\left|\frac{P - P_i}{2\,P_p}\right|^{r-1}\right] \qquad (5)$$

where β is such that $\beta(P_p/\Delta_p)$ is the slope of the unloading curve. As the flanges of a beam buckle and the member becomes somewhat less stiff the value of β decreases. For example, the slope of the unloading curve

through point A in Fig. 16 is less steep than the slope of the skeleton curve at the origin.

The behavior of β is displayed in Fig. 18 for two specimens. For a rather stiff specimen F2HS-C7 having connecting plates, β remains nearly constant throughout the test. On the other hand, for specimen F1-C6 subjected to very large amplitudes of deflection, buckling of the flanges occurs early in the experiment and continues to increase with the increasing number of cycles. Careful measurements of the rebound slopes on the hysteresis loops provide a very sensitive indication of the onset and the degree of buckling. Such refinement is usually unnecessary.

For practical applications, based on the experiments described here, the recommended parameters are $\alpha = 0.5$, $\beta = 1$, and $r = 8$ or 9.

Energy Absorption Capacity of Connections. The experimental results described above indicate the reliability of achieving substantial hysteretic loops with each plastic cycle by any one of the connections tested. Since the areas enclosed by such loops represent dissipated energy, these loops provide information on the energy absorption capacity of connections.

In going from one size amplitude of deflection to another the two halves of a hysteresis loop are not equal. Frequently this has also occurred to a less pronounced degree due to the inaccuracies of the experimental controls. For this reason, in analyzing data it was found advantageous to treat half-cycles of every hysteresis loop as the basic data. This quantity is designated here by W and represents the work or energy dissipated in plastically deforming a member per half-cycle. This dissipated energy can be compared with $1/2\ (P_p\ \Delta_p)$ the elastic energy at impending plastic load P_p. By dividing W by $P_1/2P(P_p\ \Delta_p)$ one obtains dimensionless energy ratio e per half-cycle of a hysteresis loop.

Another variable required in this discussion is the deflection plasticity ratio π_d defined in Fig. 17. This quantity is the ratio of the residual plastic deflection for each half-cycle to Δ_p. The plasticity ratio introduced here has a physical meaning similar to the ductility factor μ but does not have the disadvantage of including in it the recoverable deformation. It also gives a direct indication of the cumulative damage similar to the one commonly used in the fatigue studies of materials.

An extensive investigation of relating the dissipated energy ratio e to the plasticity ratio π_d has been made for hundreds of half-cycle hysteresis loops obtained in these experiments. This study has been reported elsewhere (6, 8). It is significant to note that the same results follow from Fig. 19. In this figure the mean or average values of e versus π_d for each one of the experiments are plotted. This procedure of analyzing the data leads to the same basic relation:

$$e = 1.77\ \pi_d \qquad (6)$$

With the exception of the point for an F3-C5 connection which had unusual hysteresis loops, Eq. 6 fits the experimental points with considerable accuracy.

The accumulated or the total energy absorbed by the members at failure is plotted against the accumulated residual plastic deflections for each half-cycle in Fig. 20. This figure provides some quantitative information on the energy absorbing capabilities of the various connections.

By performing dynamic analysis for seismic inputs on actual structures, the requirements for energy dissipation at the various joints can be determined. The results of this type of study (17) for a one-degree of freedom system are shown in Fig. 21. By measuring the area under the loops for each half-cycle the total mount of energy to be dissipated can be found. Alternatively, and much simpler, the residual plastic deflections for each half-cycle (AB + BC + CD + etc., in Fig. 21) giving the cumulative damage can be used for the same purpose. These requirements can be compared with the performance data as in Fig. 20.

Comparison of Connections. Before closing, a comparison between connections may be of interest. This is done qualitatively in Fig. 22. This self-explanatory figure emphasizes the need for selecting a basis for such a comparison. The energy absorption capabilities of connections are quite different depending on the chosen criterion.

ACKNOWLEDGEMENTS

It is a pleasure to acknowledge the financial support of several groups: NSF provided the funds to initiate this work, AISI supported the major part of the investigation, and AISC donated the two built-up specimens. As the project extended over a period of years, a number of people have participated and made significant contributions. Among these, graduate students H. A. Franklin, D. W. Murray, M. C. Chen, and D. T. Tang and undergraduate student J. V. Meyer deserve special mention. Professor V. V. Bertero's collaboration was most helpful. The two most recent tests on the built-up specimens were performed by Dr. Makoto Watabe and David T. Tang. The drawings were prepared by David Prior.

BIBLIOGRAPHY

1. Igarashi, S.; J. Sumida and J. Sakamoto, "Experimental Study on the Hysteresis Characteristics of Steel Connections with Relation to the Damping Properties of a Structure," Transactions of the Architectural Institute of Japan, Vol. 75, August 1962.

2. Naka, T ; B Kato, M. Watabe, A. Tanaka and T. Sasaki, "Research on the Behavior of Steel Beam-to-Column Connections Subjected to Lateral Force - Report No. 2," Trans. of the Arch. Inst. of Japan, Vol. 102, September 1964.

3. Naka, T ; B. Kato, M. Watabe, A. Tanaka and T. Sasaki, "Research on the Behavior of Steel Beam-to-Column Connections Subjected to Lateral Force - Report No. 3," Trans. of the Arch. Inst. of Japan, Vol. 103, October, 1964.

4. Bertero, Vitelmo, "Inelastic Behavior of Beam-to-Column Subassemblages Under Repeated Loading," Report No. EERC 68-2, Earthquake Engineering

Research Center, University of California, April 1968.

5. Carpenter, L. D. and L. W. Lu, "Behavior of Steel Frames Under Repeated Loading," Report No. 332.2, Fritz Engineering Laboratory, Lehigh University, February 1968.

6. Popov, E. P. and R. B. Pinkney, "Behavior of Steel Building Connections Subjected to Repeated Inelastic Strain Reversal," Report No. SESM 67-30, Structural Engineering Laboratory, Univ. of Calif., Berkeley, December 1967.

7. Popov, E. P. and R. B. Pinkney, "Behavior of Steel Building Connections Subjected to Repeated Inelastic Strain Reversal - Experimental Data," Report No. SESM 67-31, Structural Engineering Laboratory, Univ. of California, Berkeley, December 1967.

8. Popov, E. P. and R. B. Pinkney, "Alternating Inelastic Strains in Steel Connections," J. of Structural Division, ASCE, (in preparation)

9. Hanson, R. D., "Comparison of Static and Dynamic Hysteresis Curves," J. of the Engineering Mechanics Division, ASCE, Vol. 92, No. EM5, Proc. Paper 4949, October 1966, pp. 87-113.

10. Rea, D.; R. W. Clough, J. G. Bouwkamp and U. Vogel, "Damping Capacity of a Model Steel Structure," Proceedings 4WCEE.

11. Morrow, JoDean, "Cyclic Plastic Strain Energy and Fatigue of Metals," Internal Friction, Damping and Cyclic Plasticity, ASTM, STP-378, 1965, p. 77.

12. Ramberg, W. and W. R. Osgood, "Description of Stress-Strain Curves by Three Parameters," Technical Note 902, NACA, July 1943.

13. Kaldjian, M. J., "Moment-Curvature of Beams as Ramberg-Osgood Functions," Journal of the Structural Division, ASCE, Vol. 93, No. ST5, Proc. Paper 5488, October 1967, pp. 53-65.

14. Popov, E. P., "Low-Cycle Fatigue of Steel Beam-to-Column Connections," International Symposium on the Effect of Repeated Loading on Materials and Structures, RILEM-Instituto de Ingeneria, Vol. VI, Mexico City, September 1966.

15. Masing, G., "Eigenspannungen and Verfestigung beim Messing," Proceedings of the Second International Congress for Applied Mechanics, Zurich, September 1926.

16. Jennings, Paul C., "Periodic Response of a General Yielding Structure," J. of the Engineering Mechanics Division, ASCE, Vol. 90, No. EM2, Proc. Paper 3871, April 1964, pp. 131-166.

17. Berg, G. V., "A Study of the Earthquake Response of Inelastic Systems," Proceedings, Structural Engineers Association of California, October 1965.

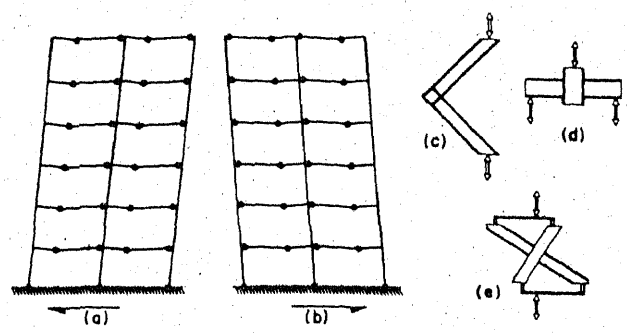

FIG. 1 SCHEMATIC BEHAVIOR OF A FRAME IN AN EARTHQUAKE AND EXPERIMENTAL IDEALIZATIONS OF ITS COMPONENTS.

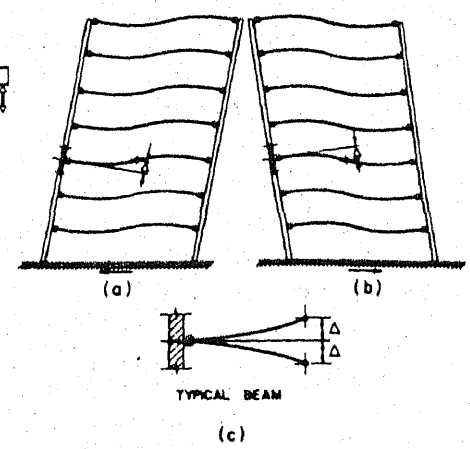

FIG. 2 ASSUMED FRAME BEHAVIOR FOR SELECTION OF A SPECIMEN

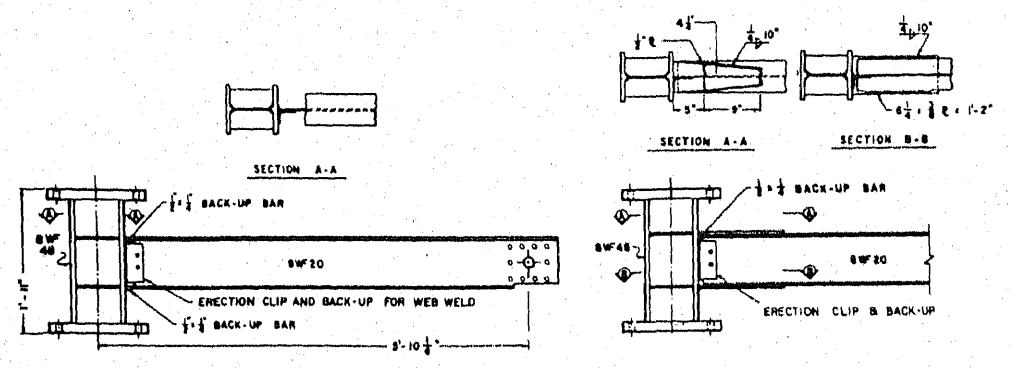

(a) TYPE F1 WELDED CONNECTION (b) TYPE F2 WELDED CONNECTION

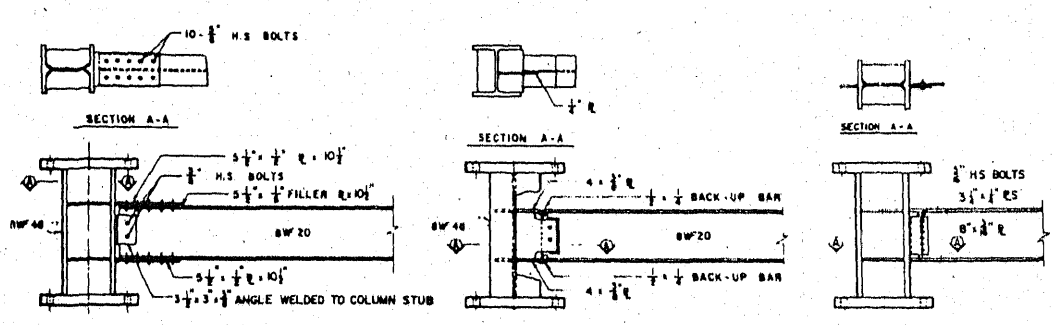

(c) TYPE F3 H.S BOLTED CONNECTION (d) TYPE W1 WELDED CONNECTION (e) TYPE LA1

FIG. 3 TEST SPECIMENS

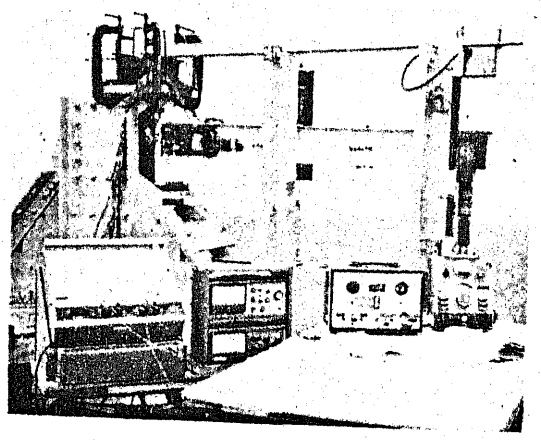

FIG. 4 GENERAL VIEW OF THE EXPERIMENT

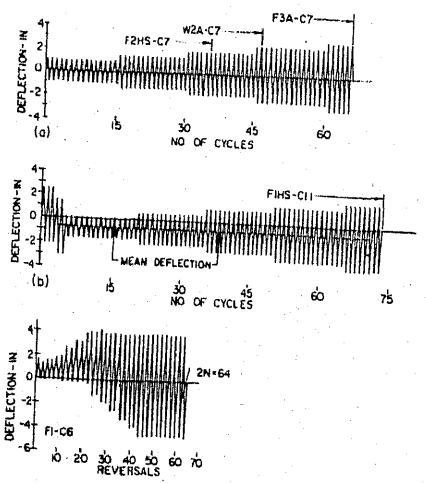

FIG. 5 EXAMPLES OF CYCLING SEQUENCE

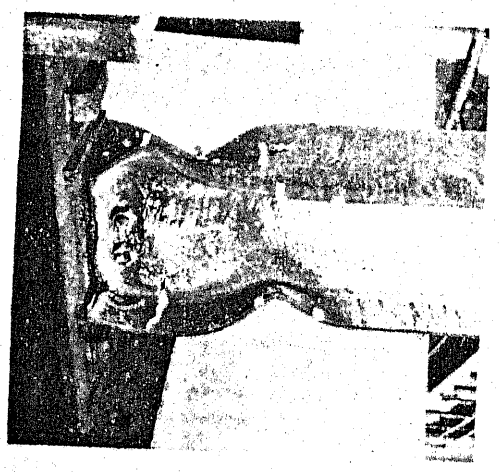

FIG. 6 F1-C6

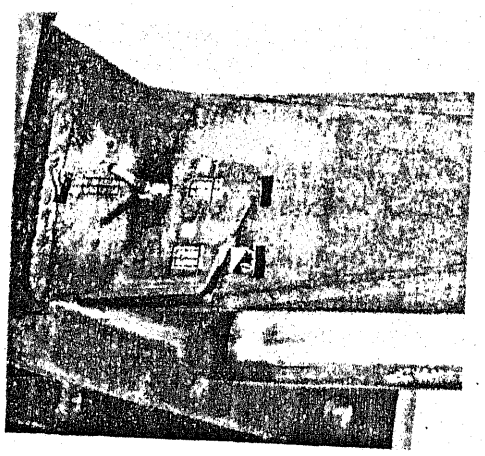

FIG. 7 F2-C4

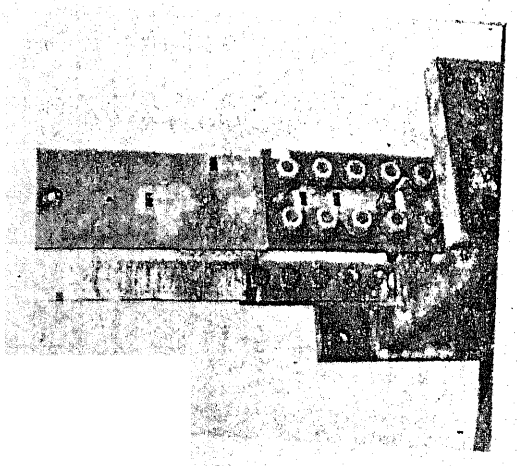

FIG. 8 F3A-C7

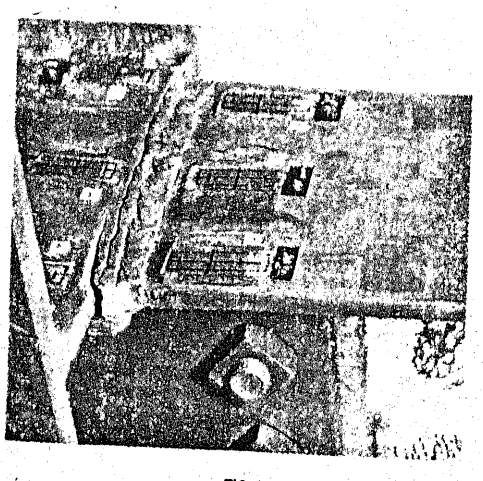

FIG. 9 W1-C7

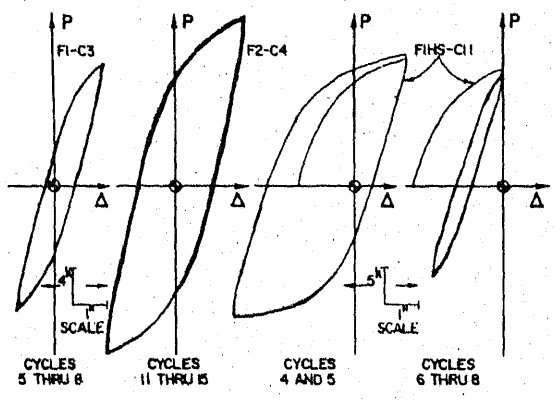

FIG. 10 TYPICAL LOAD-DEFLECTION HYSTERESIS LOOPS

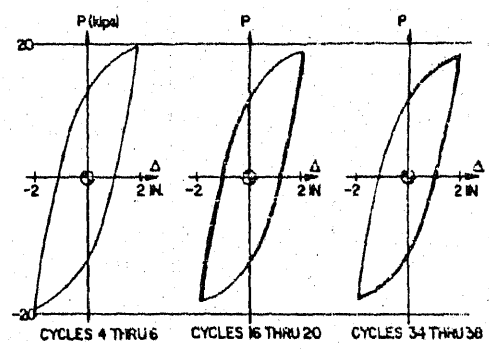

FIG. 11 CYCLIC SOFTENING OF HYSTERESIS LOOPS AT CONSTANT DEFLECTION SPECIMEN F2-C4

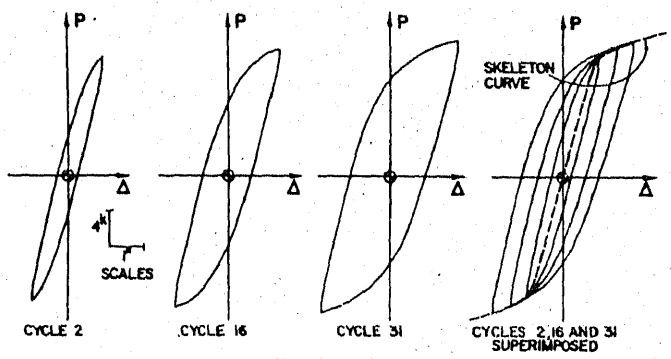

FIG. 12 ENLARGEMENT OF LOAD-DEFLECTION HYSTERESIS LOOPS WITH INCREASING LOAD. SPECIMEN W1-C7

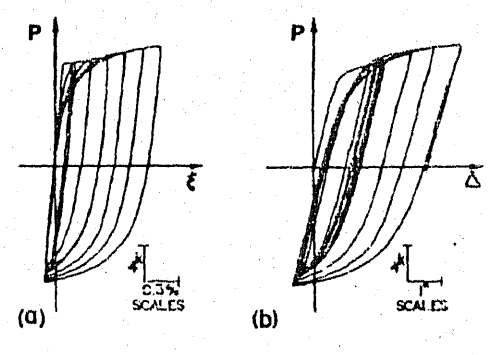

FIG. 13 LOAD-STRAIN AND LOAD-DEFLECTION HYSTERESIS LOOPS. SPECIMEN F1-C6

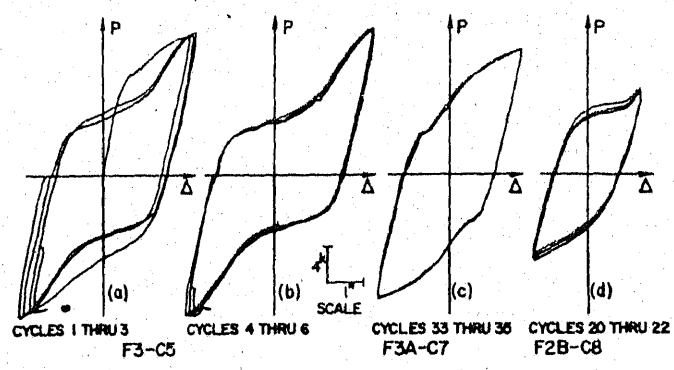

FIG. 14 LOAD-DEFLECTION HYSTERESIS LOOPS

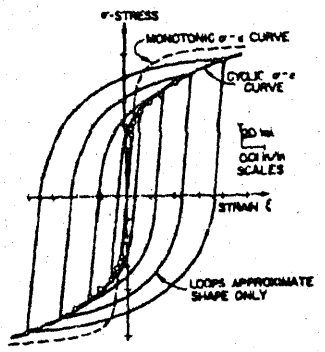

FIG. 15 MONOTONIC AND CYCLIC STRESS-STRAIN BEHAVOIR OF SAE 4340 STEEL (AFTER MORROW)

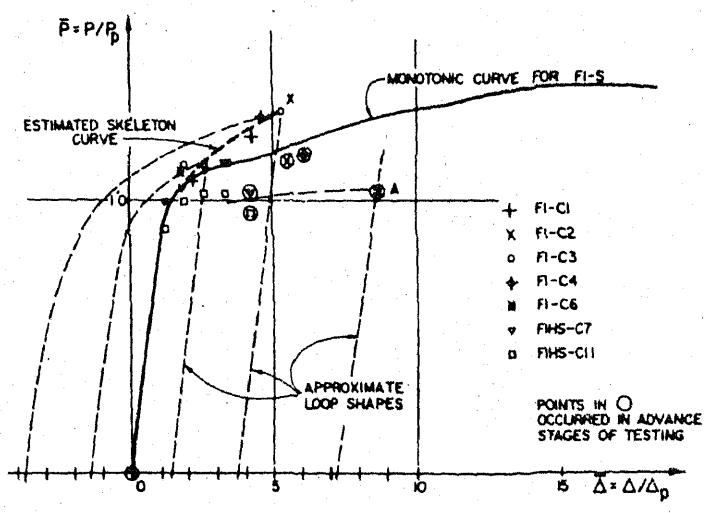

FIG. 16 MONOTONIC AND CYCLIC LOAD-DEFLECTION CURVES

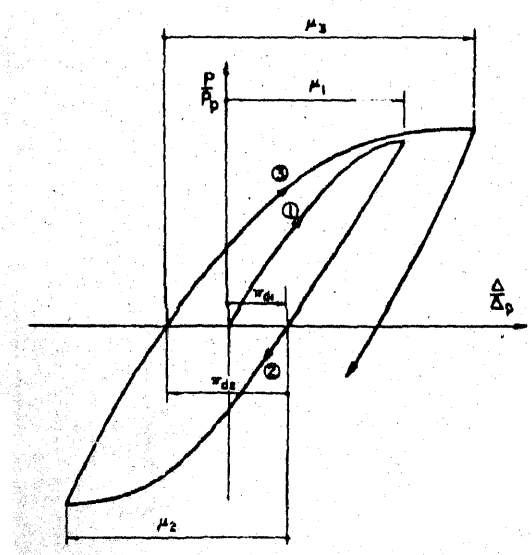

FIGURE 17 - DEFINITION OF DUCTILITY FACTOR μ AND PLASTICITY RATIO π_d

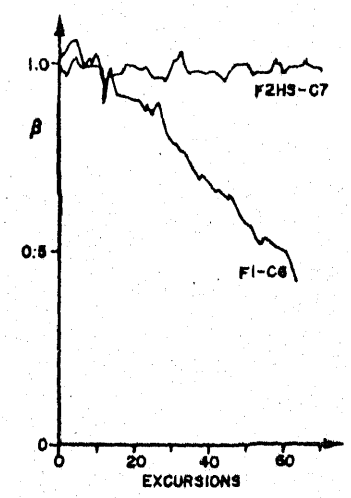

FIG. 18 SLOPE FACTOR β

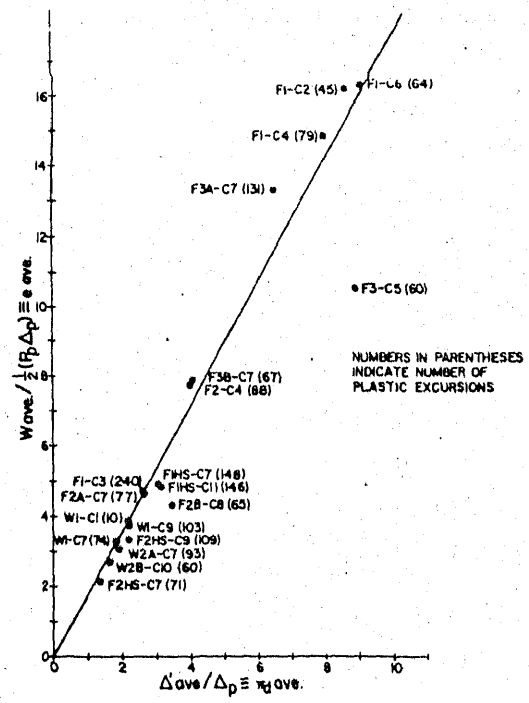

FIG. 19 AVERAGE ENERGY RATIO VERSUS AVERAGE PLASTICITY RATIO

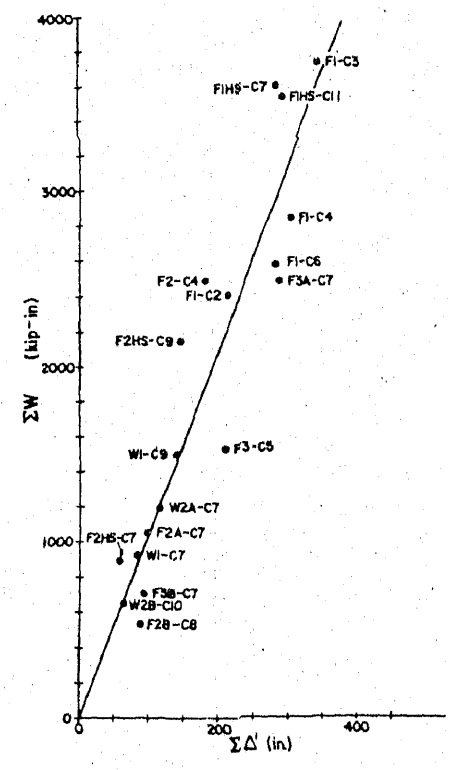

FIG. 20 ACCUMULATED ENERGY VERSUS ACCUMULATED Δ'

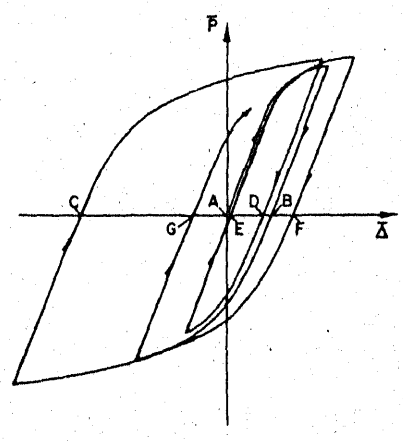

FIG. 21 RESPONSE OF AN INELASTIC SYSTEM TO A DYNAMIC INPUT (AFTER G. BERG)

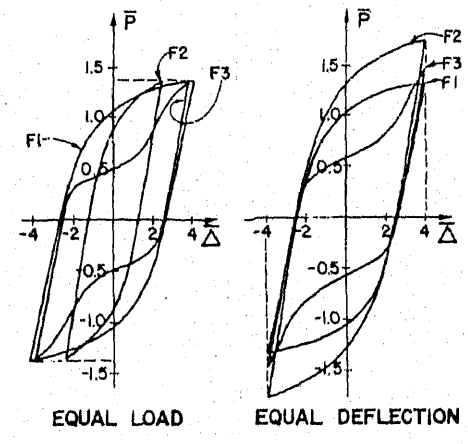

FIG. 22 QUALITATIVE COMPARISON OF ENERGY ABSORPTION OF TYPICAL CONNECTIONS ON DIFFERENT BASES

TABLE I

Specimen	Cycles to Failure	Type of Cycling Number of Cycles at Given Tip Deflection*
F1-C1	28	5 at ± 1 in.; 5 at ± 2 in.; 10 at ± 3 in.; 8 at ± 4 in.
F1-C2	22½	22½ at ± 3 in.
F1-C3	120	100 at ± 1 in.; 20 at ± 3 in.
F1-C4	39 ½	20 at ± 2 in.; 19½ at ± 3 in.
F1-C6	32	5 at ± 3/4 in.; 5 at ± 1½ in.; 10 at ± 1½ in. to ± 4 in.; 12 at ± 4 in.
F2-C1	18	5 at ± 1 in.; 5 at ± 1½ in.; 8 at ± 3 in.
F2-C4	44	42 at ± 1½ in.; 2 at ± 2 in.
F2A-C7	38 ½	15 at ± 3/4 in.; 15 at 1¼ in.; 8½ at ± 1-3/4 in.
F2B-C8	32 ½	15 at ± 3/4 in.; 15 at ± 1¼ in.; 2½ at ± 1-3/4 in.
F3-C1	9 ½	5 at ± 2½ in.; 4½ at ± 4 in.
F3-C5	30	30 at approximately ± 2½ in.
F3A-C7	65 ½	15 at ± 3/4 in.; 15 at ± 1¼ in.; 15 at ± 1-3/4 in.; 15 at ± 2¼ in.; 5½ at ± 3 in.
F3B-C7	33 ½	15 at ± 3/4 in.; 15 at ± 1¼ in.; 3½ at ± 1-3/4 in.
W1-C7	37	15 at ± 3/4 in.; 15 at ± 1¼ in.; 7 at ± 2 in.
** W1-C9	51 ½	2 at ± 1-3/4 in.; 15 at ± 3/4 in.; 15 at ± 1¼ in.; 15 a ± 1-3/4 in.; 4½ at ± 2¼ in.
W2A-C7	46 ½	15 at ± 3/4 in.; 15 at ± 1¼ in.; 15 at ± 1-3/4 in.; 1½ at ± 2¼ in.
W2B-C10	30	5 at ± 1-3/4 in.; 15 at ± 3/4 in.; 10 at ± 1¼ in.
F1HS-C7	74	15 at ± 3/4 in.; 15 at ± 1¼ in.; 15 at ± 1-3/4 in.; 15 at ± 2¼ in.; 14 at ± 2-3/4 in.
F1HS-C11	73	5 at ± 2¼ in.; 15 at ± 3/4 in.; 15 at ± 1¼ in.; 15 at ± 2¼ in.; 14 at ± 2-3/4 in.
F2HS-C7	35 ½	15 at ± 3/4 in.; 15 at ± 1¼ in.; 5½ at ± 1-3/4 in.
F2HS-C9	54 ½	2 at ± 1-3/4 in.; 15 at ± 3/4 in.; 15 at ± 1¼ in.; 15 at ± 1-3/4 in.; 7½ at ± 2¼ in.

* Tip deflections are approximate, and are measured from mean position.
** Results from two defectively fabricated W1 specimens are not included.

TABLE II

Specimen	Cycles to Failure	Type of Cycling Number of Cycles at Given Tip Deflection*
LA1-C12	43 ½	15 at ± ½ in.; 2 at ± 1 in.; 5 at ± 3/4 in.; 10 at ± 1 in.; 10 at ± 1 ½ in.; 1 ½ at ± 2 in.
LA2-C12	43	15 at ± ½ in.; 2 at ± 1 in.; 5 at ± 3/4 in.; 10 at ± 1 in.; 10 at ± 1 ½ in.; 1 at ± 2 in.

* Subtract approximately 1/16 in. from deflections given to account for support rotation.
In these experiments P max. was approximately 7 kips.